Université Grenoble Alpes — LEGI

Master 2 TMA — Advanced Experimental Methods

Laboratory Report

Active grid generated turbulence in a wind tunnel

(with three additional laboratory studies)

Author: **Mahmoud Bechki**

Academic year: 2025–2026

Grenoble, France

Abstract (English)

This report groups four laboratory experiments from the M2 TMA advanced experimental methods module. The main experiment looks at turbulence measured downstream of a grid inside a wind tunnel, and compares an active protocol to an open static configuration using hot wire anemometry. I describe the setup, what the sensors actually measure, and the analysis applied to the velocity signals. The focus is on simple but solid tools: turbulence intensity, probability density functions, and power spectra computed with the Welch method. I then connect the observations to the usual picture of homogeneous isotropic turbulence and to the discussion around equilibrium versus nonequilibrium cascades reported for active grid flows. Three additional studies are also presented: spectral analysis of a turbulent wake behind a circular cylinder using a Cobra probe, vibrational response and wave dynamics in an elastic plate using time frequency plots, and the near field dynamics of a two fluid atomizer in the Spray Bank experiment.

Résumé (Français)

Ce compte rendu regroupe quatre travaux pratiques du module de méthodes expérimentales avancées (M2 TMA). Le TP principal étudie une turbulence mesurée en aval d une grille dans une soufflerie, avec une comparaison entre un protocole de grille active et une configuration grille ouverte statique, à l aide d une anémométrie à fil chaud. Je présente la configuration expérimentale, ce que les capteurs mesurent, puis l analyse appliquée aux signaux de vitesse. L accent est mis sur des outils simples mais robustes: intensité turbulente, fonctions de densité de probabilité, et spectres de puissance calculés avec la méthode de Welch. Je relie ensuite les observations à l image classique de turbulence homogène isotrope et à la discussion sur les cascades en équilibre ou hors équilibre rapportées pour les grilles actives. Trois autres études sont aussi présentées: analyse spectrale du sillage turbulent derrière un cylindre avec une sonde Cobra, réponse vibratoire et dynamique d ondes dans une plaque élastique via des cartes temps fréquence, et dynamique proche champ d un atomiseur bi fluide dans l expérience Spray Bank.

AI usage statement.
AI tools were used only for language correction and formatting, and for clarifying general theoretical concepts already covered in the course material. No AI-generated content was used for scientific analysis, results, figures, or interpretation.

Contents

1 General introduction and shared analysis tools **3**

2 Part I — Main TP (0): Active grid generated turbulence in a wind tunnel **3**
2.1 Introduction and objectives 3
2.2 Experimental configuration 3
2.3 Measurement principles 4
2.4 Analysis methods 5
2.5 Results 6
2.6 Discussion 8
2.7 Conclusion (main TP) 8

3 Part II — Secondary laboratory studies **9**
3.1 Turbulent wake behind a circular cylinder (Soufflerie) 9
3.2 Waves in an elastic plate (Gong) 10
3.3 Spray Bank experiment: near field spray dynamics 11

4 General conclusion and perspectives **11**

A Additional notes on processing choices (main TP) **12**

1 General introduction and shared analysis tools

In all four experiments we end up with time signals, and the goal is to turn those signals into something physical and interpretable. The basic steps are always the same: split the signal into mean and fluctuations, look at statistics such as PDFs, and look at frequency content through spectra. Depending on the case, a spectrum can show a clear peak that points to a coherent mechanism, or it can be broadband which is what we expect for turbulence.

Given a measured time series $u(t)$, we write

$$u(t) = \overline{u} + u'(t), \tag{1}$$

where $\overline{u}$ is the time average and $u'(t)$ the fluctuation. A basic measure of fluctuation level is the turbulence intensity:

$$I = \frac{u'_{\mathrm{rms}}}{\overline{u}}, \qquad u'_{\mathrm{rms}} = \sqrt{\overline{u'^2}}. \tag{2}$$

For advected turbulence, Taylor's hypothesis is used in a qualitative way (and with its usual limitations in mind):

$$x \simeq \overline{u}\, t, \qquad k \simeq \frac{2\pi f}{\overline{u}}. \tag{3}$$

2 Part I — Main TP (0): Active grid generated turbulence in a wind tunnel

2.1 Introduction and objectives

Grid turbulence is a clean way to get close to homogeneous isotropic turbulence in the lab. Downstream of a grid, wakes interact and merge, and we can measure fluctuations over many scales. The interesting part with an active grid is that we can force the large scales by moving blades, so the flow can reach higher turbulence levels than with a passive open grid.

In this TP, the goals are:

- characterize turbulence downstream of the grid in the wind tunnel,
- compare the active triple random protocol with the open static configuration,
- apply statistical and spectral tools on the hot wire velocity signals,
- discuss what this says about the cascade picture, and how it relates to active grid studies (Mora et al. 2019; Pope 2000).

2.2 Experimental configuration

Wind tunnel and turbulence generator

The experiment is performed in the LEGI wind tunnel test section. Turbulence is generated upstream by a grid. In the active configuration, blades rotate according to a programmable protocol, which changes the large scale structures injected into the flow. In the open configuration, the grid is static and the forcing is weaker.

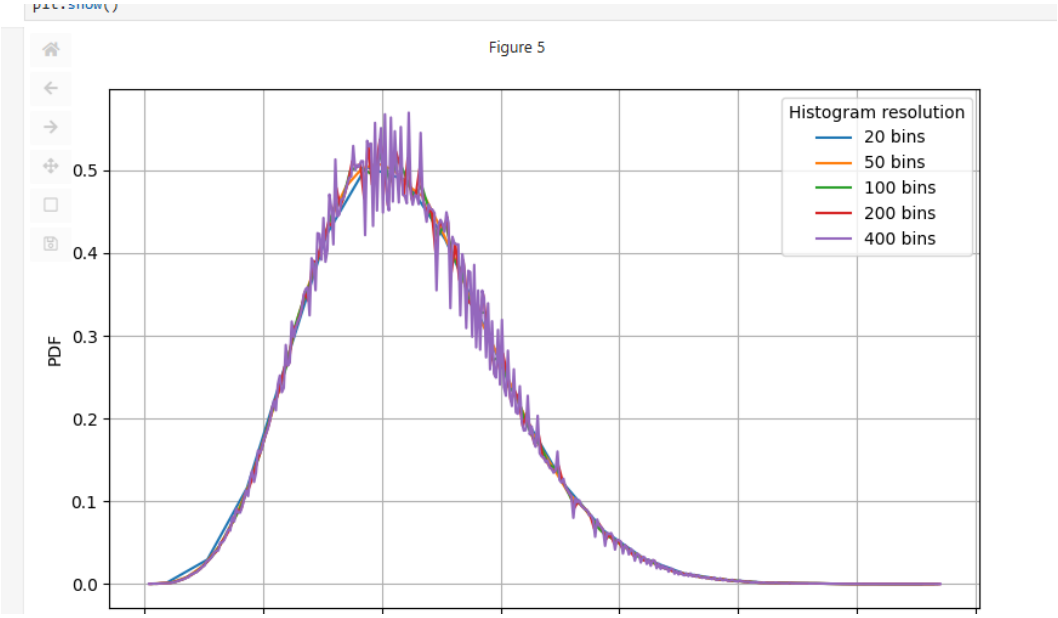

Figure 1: Wind tunnel schematic and location of the test section and grid.

Instrumentation

Hot wire anemometry (CTA). A thin overheated wire is placed in the flow. Cooling depends on the local velocity. In constant temperature mode, the electronics keep the wire temperature constant and the bridge voltage is used to infer velocity.
Pitot tube. A Pitot tube gives a reference mean velocity used for calibration through the pressure difference between stagnation and static pressure.
Traverse and positions. Measurements are done at several downstream positions x from the grid, and for different incoming speeds and protocols. The probe is placed near the centerline to avoid mean shear and stay close to HIT conditions.

2.3 Measurement principles

Calibration: King law

The hot wire voltage E is related to velocity through a calibration curve usually modeled by King law:

$$E^2 = A + B\,U^n, \tag{4}$$

with A, B, and n obtained from a fit using Pitot reference values. After calibration, the voltage signal is converted into $u(t)$.

Mean and fluctuations

We use

$$u(t) = \overline{u} + u'(t), \tag{5}$$

where $\overline{u}$ is the time average over the record and $u'(t)$ contains the turbulent fluctuations.

Taylor hypothesis

When the mean advection dominates, we can interpret time as space in a qualitative way:

$$x \approx \overline{u}\, t, \qquad k \approx \frac{2\pi f}{\overline{u}}. \tag{6}$$

2.4 Analysis methods

Turbulence intensity

A first quantity is the turbulence intensity

$$I = \frac{u'_{\mathrm{rms}}}{\overline{u}}, \qquad u'_{\mathrm{rms}} = \sqrt{\overline{u'^2}}. \tag{7}$$

PDFs and Gaussian reference

PDFs let us see how the measured values are distributed. Comparing to a Gaussian with the same mean and variance is a simple way to see if the signal behaves like a normal random process or if it has asymmetry and heavy tails.

Power spectra and Welch method

To study how energy is distributed across frequencies, I compute the PSD using the Welch method. This matters because the spectrum can change noticeably depending on how we segment and average the data. In an ideal inertial range, Kolmogorov scaling suggests a $k^{-5/3}$ trend for the one dimensional spectrum (Pope 2000):

$$\Phi_u(k) \propto \varepsilon^{2/3}\, k^{-5/3}, \tag{8}$$

but in practice the observable range depends on Reynolds number and measurement limits.

Integral scale from autocorrelation

The normalized autocorrelation is

$$R_{uu}(\tau) = \frac{\overline{u'(t)\, u'(t+\tau)}}{\overline{u'^2}}. \tag{9}$$

An integral time scale can be estimated by integrating R_{uu} up to the first zero crossing, and turned into an integral length scale using Taylor hypothesis:

$$L \approx \overline{u} \int_0^{\tau_0} R_{uu}(\tau)\, d\tau. \tag{10}$$

Dissipation estimate and small scales

Assuming local isotropy, dissipation can be linked to longitudinal gradients:

$$\varepsilon \approx 15\nu \left(\frac{\partial u'}{\partial x}\right)^2, \qquad \frac{\partial}{\partial x} \approx \frac{1}{\overline{u}} \frac{\partial}{\partial t}. \tag{11}$$

Then the Kolmogorov and Taylor scales are

$$\eta = \left(\frac{\nu^3}{\varepsilon}\right)^{1/4}, \qquad \lambda = \sqrt{\frac{15\nu\,\overline{u'^2}}{\varepsilon}}. \tag{12}$$

A useful Reynolds number is

$$Re_\lambda = \frac{u'_{\mathrm{rms}}\lambda}{\nu}. \tag{13}$$

Dissipation coefficient

A nondimensional measure often used to discuss cascade regimes is

$$C_\varepsilon = \frac{\varepsilon L}{u'^3_{\mathrm{rms}}}. \tag{14}$$

In equilibrium cascade conditions, it is expected to approach a constant at high Reynolds numbers, while active grid turbulence can show different trends depending on the regime (Mora et al. 2019).

2.5 Results

PDF robustness: sensitivity to binning

Figure 2 shows the estimated PDF for different histogram resolutions. This is a simple check, but it is important, because otherwise the observed PDF shape could come from the chosen binning rather than from the signal itself.

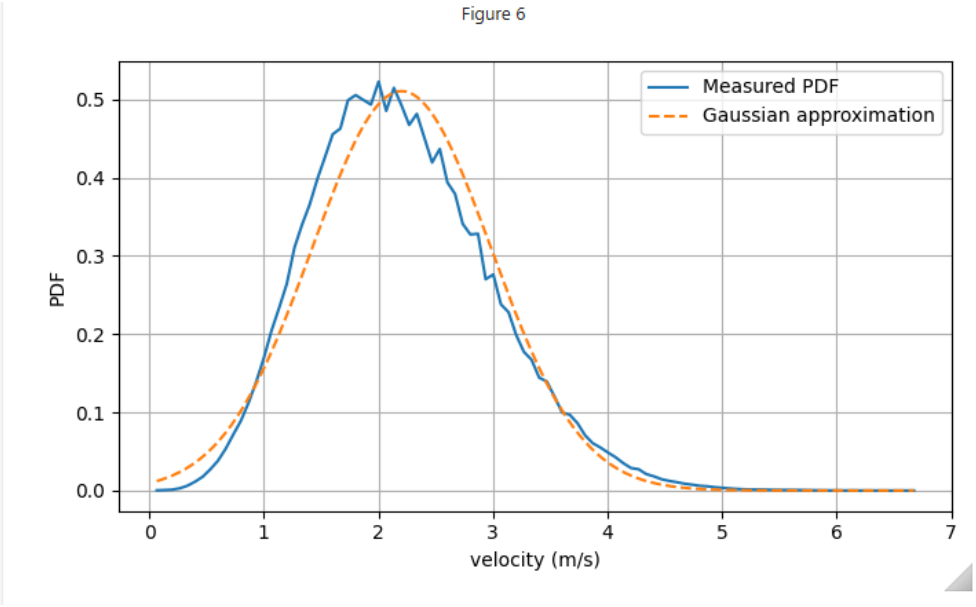

Figure 2: Estimated PDF of velocity for different histogram resolutions.

Gaussian comparison

Figure 3 compares the measured PDF with a Gaussian approximation based on the same mean and variance. The difference between both curves shows that the signal is not perfectly Gaussian.

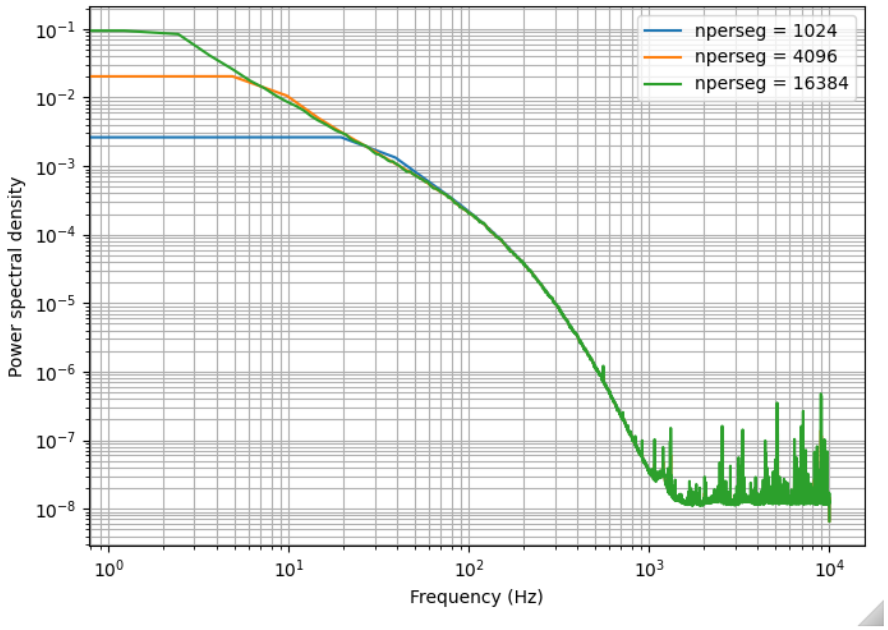

Figure 3: Measured velocity PDF compared with a Gaussian approximation.

PSD robustness: sensitivity to Welch parameters

Figure 4 shows the PSD computed with different Welch segment lengths. You can clearly see the tradeoff between smoothness and frequency resolution. This plot is useful since it helps justify the PSD settings used later for interpretation.

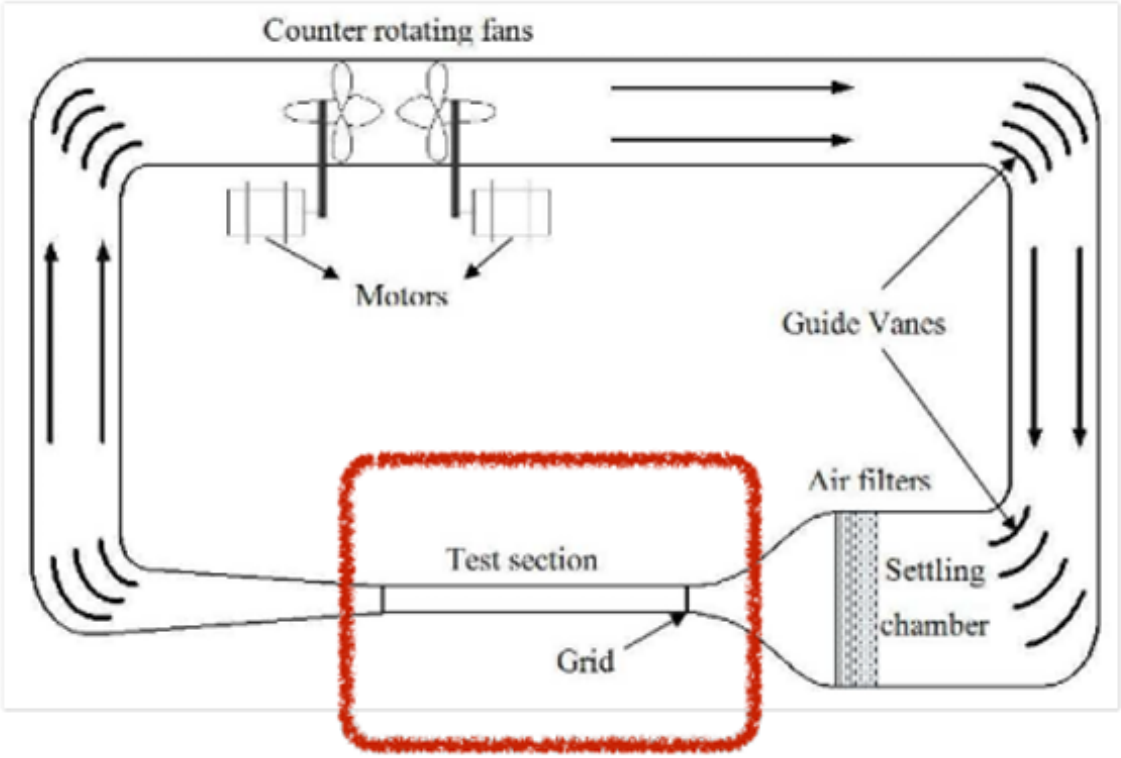

Figure 4: Power spectral density of velocity fluctuations and sensitivity to the Welch parameter n_{perseg}.

2.6 Discussion

What the PDFs tell us

Seeing a non Gaussian PDF is not surprising in turbulence. It can come from intermittent events, coherent structures, or simply the fact that we are at finite Reynolds numbers and not in an ideal limit. The point is that the Gaussian curve is a useful baseline, and the measured deviation is a real feature of the signal.

What the PSD tells us

The PSD gives a scale by scale view. The low frequency range corresponds to large scale motions injected by the grid. Higher frequencies correspond to smaller scales and dissipative effects, although part of this range can also be affected by measurement noise. The sensitivity study also tells us how careful we need to be with spectral estimation, because the method settings can change the appearance of the curve.

Link with cascade ideas

In an ideal picture, one would like to identify a range compatible with the usual cascade scaling. In practice, whether we can see a clean inertial range depends on Reynolds number, on how good Taylor hypothesis is, and on measurement bandwidth. In active grid flows, an important point is that the cascade can behave differently depending on whether it is in equilibrium or not, and that is why nondimensional dissipation measures like C_ε are often used (Mora et al. 2019). Here, with the plots we have, the strongest statement we can make is based on robust statistics and robust spectra.

2.7 Conclusion (main TP)

This TP gave a clean dataset of velocity signals downstream of a grid in a wind tunnel. The analysis focused on robust steps: checking PDF stability, comparing to a Gaussian baseline, and computing PSDs with a justified choice of Welch parameters. Overall, these results are consistent with the expected behavior of grid turbulence and provide a solid base for deeper analysis of integral scales and dissipation in the active grid framework.

3 Part II — Secondary laboratory studies

3.1 Turbulent wake behind a circular cylinder (Soufflerie)

This experiment studies the turbulent wake produced behind a circular cylinder in a wind tunnel. Velocity is measured using a fixed three component Cobra probe, giving time signals for the streamwise and transverse components. Measurements are performed at several positions in the wake. The signals are long enough to compute reliable spectra and compare how the wake behaves in space.

Physics. The cylinder forces boundary layers to develop and then separate under an adverse pressure gradient. The near wake is strongly inhomogeneous and the most visible mechanism is periodic vortex shedding. At the same time, there is broadband turbulence coming from the separated shear layers and the wake mixing. Spectral analysis is a good tool here because it can separate coherent periodic dynamics from broadband turbulence.

Analysis and result. I apply Reynolds decomposition to isolate fluctuations and then compute PSDs using the Welch method. The PSDs show a dominant low frequency peak observed at all measured positions. Its frequency is nearly constant but the amplitude changes with position, which matches the expected spatial structure of the vortex street. At higher frequencies, the energy becomes broadband and decays. The shedding frequency can be linked to the Strouhal number $St = fD/U_0$ (Brun et al. 2008).

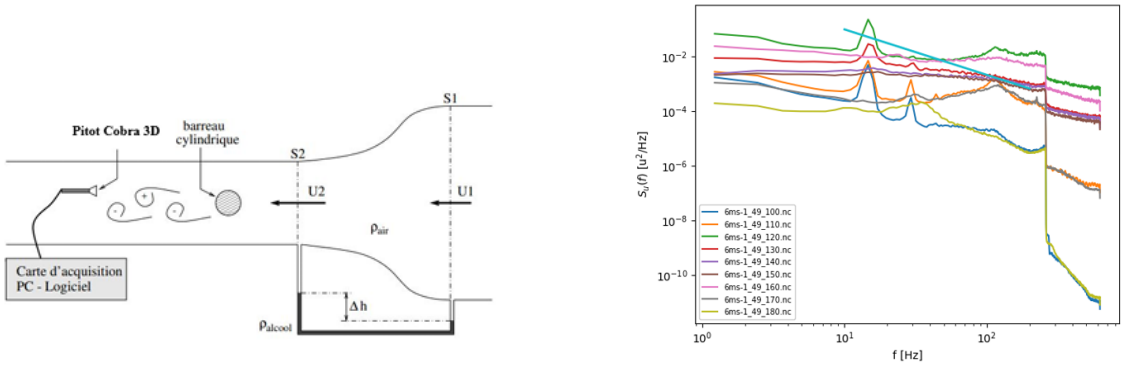

(a) Experimental setup and instrumentation with Cobra probe and acquisition.

(b) PSD $S_u(f)$ at several wake positions showing a dominant shedding peak.

Figure 5: Cylinder wake study: setup and main spectral result.

3.2 Waves in an elastic plate (Gong)

This experiment focuses on waves and vibrations in an elastic plate, using a gong as the test object. The plate is hit one or several times and the response is recorded. The goal is to see how energy is distributed in frequency and how it evolves after impacts.

Physics. When an elastic plate is excited, its response can be written as a sum of modes. Each mode has a resonance frequency and a damping rate. The geometry and material properties set the mode shapes, and damping controls how fast the energy decays. When impacts become stronger or repeated, the response can show richer interactions between modes, and energy can spread across a wider range of frequencies (Mordant 2010).

Result. The time frequency plots show clear frequency bands that correspond to resonant behavior. When the number of impacts increases, the energy level increases and the time frequency map becomes more populated, which is consistent with stronger excitation and more visible mode coupling.

(a) Experimental setup: elastic metallic plate suspended and instrumented.

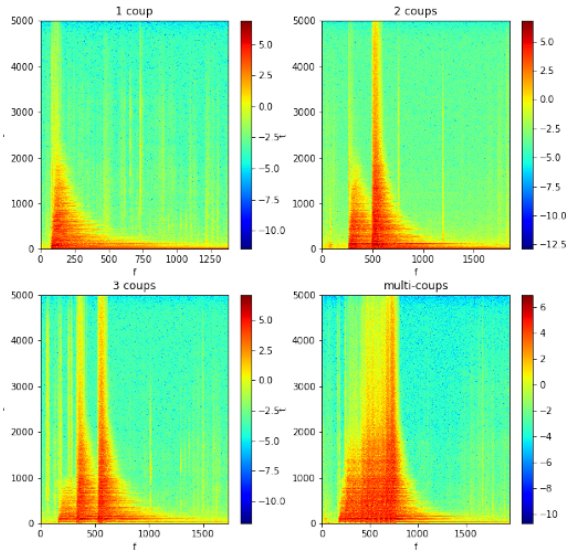

(b) Time frequency representation for different excitation conditions.

Figure 6: Gong waves: setup and main time frequency result.

3.3 Spray Bank experiment: near field spray dynamics

This experiment characterizes the near field dynamics of a liquid spray produced by a two fluid coaxial atomizer. The idea is to see how the gas liquid interaction, and especially swirl, changes the structure of the spray close to the injector.

Setup. Water is injected through a central nozzle with diameter $d_l = 2\,\text{mm}$, while air is injected through an outer annular nozzle with diameter $d_g = 10\,\text{mm}$. The gas can be injected tangentially to add swirl. The liquid flow is kept laminar and the gas flow rate is varied to change the gas liquid momentum ratio. The spray is visualized in the near field using high speed shadowgraphy.

Physics. At the injector exit, the liquid first forms a coherent liquid core. Aerodynamic shear at the gas liquid interface destabilizes the core. If the gas momentum increases, or if swirl is added, shear becomes stronger and the breakup happens earlier. So the spray dynamics contain a mix of coherent motions of the core and more irregular fluctuations linked to droplet formation (Machicoane et al. 2020).

Measurement and analysis. A key quantity is the liquid core length L_b extracted from images. Looking at $L_b(t)$ and its statistics helps quantify the unsteadiness. PDFs and autocorrelation can be used to extract typical ranges and time scales, and spectra can highlight dominant frequencies linked to oscillations or periodic breakup events.

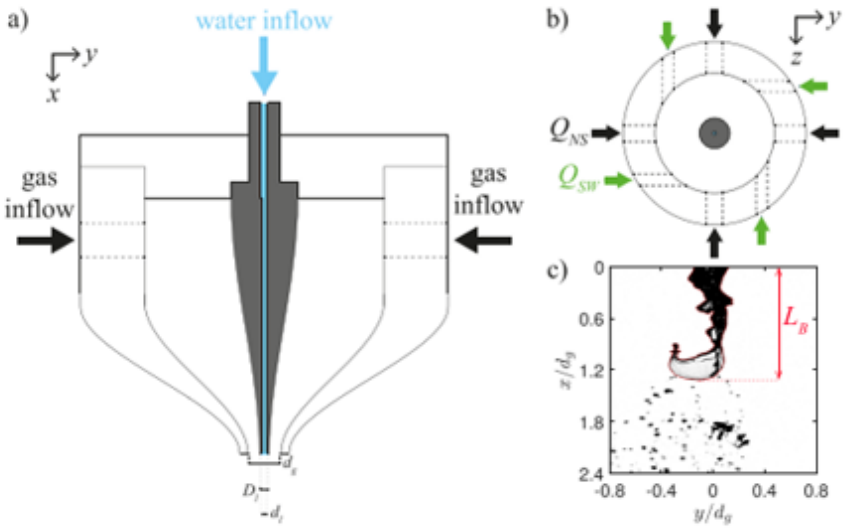

Figure 7: Spray Bank: coaxial atomizer schematic and illustration of near field breakup with liquid core length L_b.

4 General conclusion and perspectives

These four experiments show how far you can go with a good measurement and a clean signal processing workflow. In the main wind tunnel TP, PDFs and PSDs gave a solid statistical and spectral description, and I included robustness checks to justify the processing choices. In the cylinder wake, the spectrum clearly isolated the shedding peak on top of broadband turbulence. In the gong experiment, time frequency maps made the resonant bands obvious and showed how the response changes with excitation. In the Spray Bank experiment, the liquid core length is a simple but strong observable that links operating conditions to breakup dynamics.

For improvements, it would be useful to add uncertainty estimates, repeat runs for better statistics, and go deeper into nondimensional comparisons across operating conditions when possible.

References

Brun, C. et al. (2008). "Coherent Structures and their Frequency Signature in the Separated Shear Layer on the Sides of a Square Cylinder". In: *Flow, Turbulence and Combustion* 81, pp. 97–114.

Machicoane, N. et al. (2020). "Influence of steady and oscillating swirl on the near field spray characteristics in a two fluid coaxial atomizer". In: *International Journal of Multiphase Flow* 129, p. 103318.

Mora, D. O. et al. (2019). "Energy cascades in active grid generated turbulent flows". In: *Physical Review Fluids* 4.10, p. 104601.

Mordant, N. (2010). "Fourier analysis of wave turbulence in a thin elastic plate". In: *The European Physical Journal B* 76, pp. 537–545.

Pope, Stephen B. (2000). *Turbulent Flows*. Cambridge University Press.

Appendix A Additional notes on processing choices (main TP)

For the main TP, it is important to report the sampling frequency, record length, and the exact Welch settings used for spectra. For PDFs, it is also worth reporting the bin choice and showing that the PDF shape is stable when changing bin resolution. Stationarity checks and calibration uncertainty are also good points to mention briefly.